35th Annual International Conference of the IEEE EMBS
Osaka, Japan, 3 - 7 July, 2013

Sub-mm Functional Decoupling of Electrocortical Signals through Closed-Loop BMI Learning

P. Ledochowitsch, *Student Member, IEEE*, A. C. Koralek, *Student Member, IEEE*, D. Moses, J. M. Carmena, *Senior Member, IEEE* and M. M. Maharbiz, *Senior Member, IEEE*

Abstract— **Volitional control of neural activity lies at the heart of the Brain-Machine Interface (BMI) paradigm. In this work we investigated if subdural field potentials recorded by electrodes < 1mm apart can be decoupled through closed-loop BMI learning. To this end, we fabricated custom, flexible microelectrode arrays with 200 μm electrode pitch and increased the effective electrode area by electrodeposition of platinum black to reduce thermal noise. We have chronically implanted these arrays subdurally over primary motor cortex (M1) of 5 male Long-Evans Rats and monitored the electrochemical electrode impedance in vivo to assess the stability of these neural interfaces. We successfully trained the rodents to perform a one-dimensional center-out task using closed-loop brain control to adjust the pitch of an auditory cursor by differentially modulating high gamma (70-110 Hz) power on pairs of surface microelectrodes that were separated by less than 1 mm.**

I. Introduction

At cellular length scale, neurons constitute discrete functional units that are readily decoupled in a closed-loop Brain-Machine Interface (BMI) setting [1]. Likewise, volitional activity control of large brain areas (e.g. motor cortex vs. visual cortex) has been established through EEG-based BMI [2]. However, volitional decoupling of mesoscale activity on the order of a single (or of a few) cortical column (100s to 1000s of microns), as well as the optimal size and nature of such hypothetically controllable functional domains, remains highly debated.

Electrocorticography (ECoG), the measurement of electrical potentials on the surface of the cerebral cortex, is uniquely suited to investigate such mesoscopic cortical length scales. In as early as 1972 Brindley and Craggs reported a correlation between voluntary movement and ECoG signals [3]. Recently, the BMI community has developed a pronounced interest in ECoG-based BMIs for the neural control of high performance motor and communication prostheses because ECoG provides higher spatial resolution that EEG and causes less damage to neural tissue than penetrating micro needle arrays. For applications in BMI, developing high fidelity ECoG grids that optimally sample the cortex could enable smaller, less invasive, implants that provide more neural activity data for precision control. Published reports on optimal grid resolution are inconsistent and highly dependent on the animal model, the type of experiment, and the analysis performed. To give a few examples: Freeman et al. estimated optimal electrode pitch to be 1.25 mm for human cortex [4], Slutzki et al. reported 0.6 mm in rat [5], Viventi et al. [6] observed functional gradients on the order of 0.5 mm in epileptic dogs, and Khodagholy et al. reported independent cortical potentials mere 60 μm apart [7].

Rouse et al. recently demonstrated that monkeys can be trained to decouple gamma activity (power of electrocortical field potentials present between 65 and 115 Hz) on arbitrarily chosen electrodes to perform a 1-dimensional center-out BMI task [8] – as opposed to functionally pre-selected electrodes commonly used in human ECoG-BMI experiments on patients who undergo pre-surgical mapping before surgical epilepsy intervention [9]. Rouse's 'output electrodes' – i.e. electrodes chosen for BMI control – were separated by more than 3 mm and placed over distinct functional areas: one over primary motor cortex (M1), the other over dorsal premotor cortex (PMd).

In this work, we are using an experimental paradigm similar to Rouse's to investigate if gamma power decoupling can be learned for output electrodes *that are separated by less than 1 mm and that are located over the same macroscopic functional area (M1)*. To this end, we have developed a custom microelectrode array (Fig. 1) with 200 μm electrode pitch (II.A.) and modified the electrode surface to lower impedance and reduce thermal noise (II.B.). We have chronically implanted the arrays over primary motor cortex (M1) of five male Long-Evans Rats and successfully trained the animals to adjust the pitch of an auditory cursor in a one-dimensional center-out task by differentially modulating high gamma (70-110 Hz) power on two surface microelectrodes. These output electrodes were preselected to exhibit a medium level of spontaneous activity and mutual correlation in the gamma band but otherwise chosen arbitrarily. This BMI task was a modification of the single-unit based control paradigm reported by Koralek *et al* [10].

*Research was supported by SRC-FCRP (MuSyC).

P. Ledochowitsch is with the Bioengineering Department, University of California, Berkeley, and with Cortera Neurotechnologies, Inc., CA 94720, USA (corresponding e-mail: pledoch@eecs.berkeley.edu).

A. C. Koralek is with the Helen Wills Neuroscience Institute, University of California, Berkeley, CA 94720, USA (e-mail: akoralek@gmail.com).

D. Moses is with the Bioengineering Department, University of California, Berkeley, CA 94720, USA, (e-mail: dmoses@berkeley.edu)

J. M. Carmena is with the Department of Electrical Engineering and Computer Sciences, and with the Helen Wills Neuroscience Institute, University of California, Berkeley, CA 94720, USA (email: carmena@eecs.berkeley.edu)

M. M. Maharbiz is with the Department of Electrical Engineering and Computer Sciences, University of California, Berkeley, CA 94720 USA (e-mail: maharbiz@eecs.berkeley.edu).

II. Low Noise Array Design

A. Array fabrication and assembly

We have designed and fabricated 10 µm thin, flexible micro-electrocorticography (µECoG) arrays (64 channels, 40 µm electrode diameter and 200 µm electrode pitch) using Parylene C as both substrate and dielectric. The conductor consisted of an evaporated metal tri-stack (10 nm Pt, 140 nm Au, 50 nm Pt) patterned by lift-off. The electrode surface was modified with low-impedance platinum black (see II.B). A micrograph of the array sensing area is shown in Fig. 1. Our custom fabrication process is described in detail elsewhere [11]. The monolithically integrated cable was thermo-compression-bonded to a fan-out printed circuit board (PCB) using anisotropic conductive film (ACF); the adaptor PCB was outfitted with two 34-pin ZIF connectors (DF30FC-34DS-0.4V, Hirose) compatible with the *ZIF-Clip*® neural recording headstage (Tucker Davis Technologies).

B. Platinum black lowers electrode impedance

A passive neural interface, modeled as an ideally polarizable electrode, compounds the acquired signals of neural origin with thermal noise (Johnson-Nyquist) [12], [13]. The square of that noise $\bar{V}^2_{\text{noise}}$ is proportional to the real part of the electrode impedance $\text{Re}(Z(f))$ [14]:

$$\bar{V}^2_{\text{noise}} = 4k_{\text{b}}T\int_B \text{Re}(Z(f))\,df \qquad (1)$$

In equation (1) k_b is the Boltzmann constant, T is the absolute temperature, f is the frequency and B is the bandwidth of the signal (typically < 1 kHz for ECoG). In order to compensate for the small geometric area of our microelectrodes, we have increased the electrochemically available electrode area by plating each electrode with platinum black [15]. Platinum black was electrochemically deposited according to the reaction equation

$$\left[\text{PtCl}_6\right]^{2-}(aq.) + 4\text{e}^- \rightarrow \text{Pt}(s) + 6\text{Cl}^-(aq.)$$

from a solution of hexachloroplatinate (Thermo Electron Corporation, Orion 010010). The grid electrodes served as cathodes and were electroplated serially using a nanoZ (White Matter, LLC) in galvanostatic mode for 45 s. The current was limited to 500 nA. We were able to decrease the electrode impedance by more than two orders of magnitude compared to evaporated platinum. A comparison between the resistive impedance of plated and nonplated electrodes (measured when immersed in phosphate-buffered saline (PBS) at 1kHz using the nanoZ), is shown in Fig. 2).

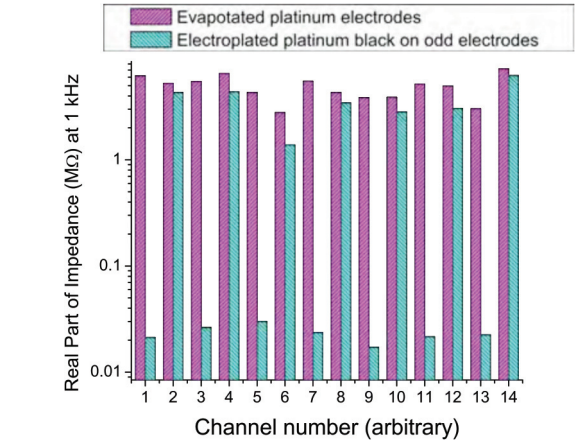

Figure 1. Impedances of plated vs. non-plated electrodes: The magenta bars show the real part of the impedance for 14 evaporated platinum electrodes. The cyan bars show impedances of the same electrodes after every odd-numbered electrode was direct current (DC) plated with platinum black for 45 s at a current of ~ -0.5 µA. Note the logarithmic resistnance scale: platinum black deposition reduced the electrode impedance by more than two orders of magnitude.

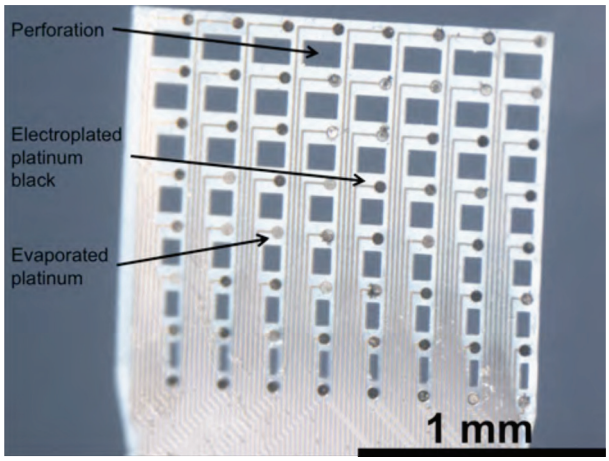

Figure 2. Optical micrograph of 64-channel, high-density µECoG: The device featured 200 µm electrode pitch, 40 µm electrode diameter and 10 µm minimum feature size (trace/space). Some of the displayed electrodes consisted of smooth and highly reflective, evaporated platinum. The black lectrodes were electrochemically plated with platinum black, a porous form of platinum that increased the effective electrochemically available area and decreases electrode impedance. Perforations in the parylene, increase the array's mechanical compliance and allow vascularization through the array.

III. Chronic Impedance Monitoring

A. Chronic implantation

All experiments were performed in compliance with the regulations of the Animal Care and Use Committees (ACUC) at the University of California, Berkeley. Five male Long-Evans rats weighing roughly 250 grams were chronically implanted with subdural 64-channel µECoG arrays (as described in II) over primary motor cortex (M1) of the right hemisphere. Stereotactic coordinates relative to bregma were used to center the arrays over M1: anteroposterior 2 mm, mediolateral 2 mm. Rats were anesthetized with Ketamine (50 mg/kg) and Xylazine (5 mg/kg) with supplemental isoflurane gas. A small craniectomy (2 mm x 3 mm) was performed, the dura

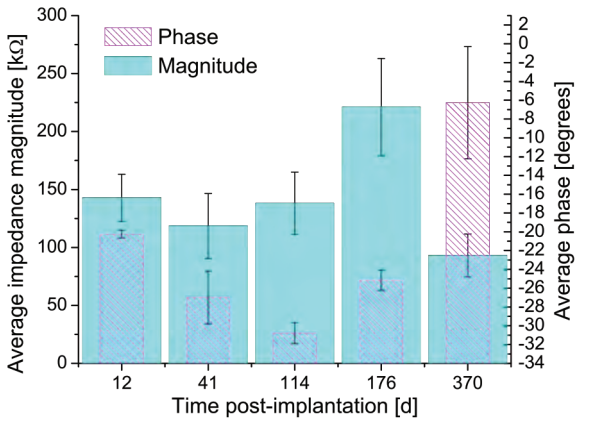

Figure 3. Time course of impedance magnitude and phase, post-implantation, averaged over the 64-μECoG electrodes. The error bars reflect the standard error of the mean. Most electrode impedance magnitudes were in the range acceptable for acquisition of surface local field potentials (< 1MΩ at 1 kHz).

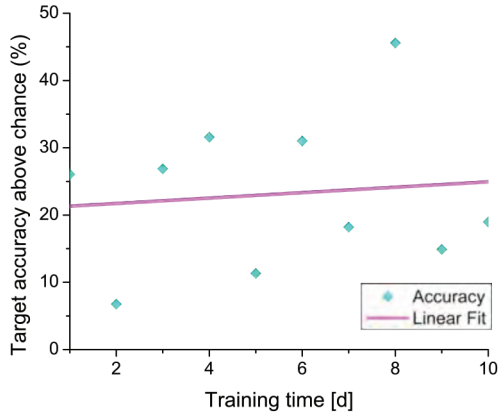

Figure 4. Target accuracy as a function of time during the learning phase: Averaged over a recording session, the animals performed the task above chance on most recording days. On average, performance improves over time but not monotonically.

removed, the array positioned on the cortex, the craniectomy covered with Gelfoam, superglue, and dental acrylic to secure the Zif-Clip connector. Scull screws placed around the craniectomy provided ground and reference, and secured the acrylic cap.

B. *In Vivo Impedance Monitoring*

In order to assess device health after implantation, we measured the electrochemical impedance at 1kHz at five different time points: 12 days, 41 days, 114 days, 176 days, and 370 days post-operatively. The measurements were performed using the nanoZ; the counter electrode was attached to the rat's tail.

Overall, we observed a slight decrease in impedance magnitude as a function of time post-implantation (Fig. 3, top). The variability of impedance magnitudes increased slightly as a function of time. Variability in electrode impedance indicates the absence of inter-electrode shorts, and can be interpreted as an absence of delamination. Most electrode impedance magnitudes were in the range acceptable for acquisition of cortical surface field potentials (< 1MΩ at 1 kHz).

Phase variability increased slightly as a function of time passed since implantation (Fig. 3, bottom).

IV. Brain Control of Auditory Cursor

Cortical field potentials were simultaneously recorded using a 64-channel Zif-Clip headstage (Tucker-Davis Technologies, ZC64) connected to a Multichannel Acquisition Processor (MAP; Plexon Inc., Dallas, TX) through a commutator. Behavioral timestamps were sent to the MAP recording system through Matlab (Mathworks, Natick, MA) and synchronized to the neural data for later analyses. All continuous data was sampled at 1 kHz.

A. *Behavioral Task*

The behavioral task was a variation of [10]. After the rodents recovered from surgery (typically 7-10 days), two low-noise microelectrodes over M1 were chosen at random given the constraint that they be 800 μm apart. The negative logarithm of gamma power (70 Hz – 110 Hz) was averaged over non-overlapping 200 ms windows and entered into an online transform algorithm that translated gamma power $P^{\gamma}(t_i)$ averaged over the i-th time window into pitch $f(t_i)$ of an auditory cursor. The specific transform used was:

$$f(t_i) = \alpha_1 \cdot P_1^{\gamma}(t_i) - \alpha_2 \cdot P_2^{\gamma}(t_i) + \beta \qquad (2)$$

where the coefficients α_1, α_2, and β were dynamically recalculated based on baseline recordings in absence of auditory feedback. Under this transform, increased activity on the first electrode produced a heightening of the cursor pitch, while increased activity on the other electrode resulted in lowering of the cursor pitch. Thus, in order to move the cursor in any one direction, the rodents had to learn to modulate gamma power on the two chosen electrodes *differentially,* as opposed to modulating bulk gamma activity in M1. The gamma power modulation had to be precise to move the cursor to one of two target pitches to obtain a target-specific reward, either in form of 20% sucrose solution or in form of a 45 mg food pellet reward. Rats were free to choose either reward in any given trial. A trial was marked incorrect if neither of these targets were achieved within 30 seconds of trial initiation. Chance levels of target achievement were estimated from daily baseline recordings, 1000 cycles long, in absence of auditory feedback.

B. *Closed loop learning performance*

At 800 μm electrode distance (center to center), the animals successfully learned to perform the BMI task significantly above chance within a single training session. Target performance was above chance on most days, and increased

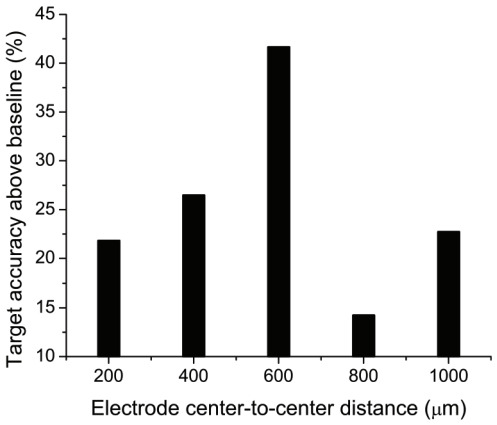

Figure 5. Target accuracy above chance as a function of distance between the 'output electrodes': The animals are able to learn controlingto control the auditory cursor even ifwith the output electrodes were adjacent, (i.e. as close to each other as 200 μm center-to-center.).

on average over time. However, the learning progress was non monotonic as is illustrated in Fig. 4.

C. Target accuracy as a function of electrode distance

We performed a variation of the experiment where we altered the electrode distance of the output electrodes (by using different electrodes on the grid) for two days at a time to test if the rats could learn alternative decoders and to investigate whether their ability to modulate gamma power differentially breaks down for electrodes that are too close together. Not only were the animals able to learn to use new pairs of output electrodes quickly, we found that the rats successfully learned to decouple gamma power on length scales as small as 200 μm (Fig. 5). The data may suggest that there exists an optimum mesoscale for control on the order of 600 μm. Such a finding would be consistent with [5] and with the scale of cortical columns proposed in literature [16]. The increased propensity to decouple activity on the length scale of a single column might be explained by lateral inhibition between adjacent columns. We have anecdotally observed that across all investigated length scales, the rats' ability to learn the BMI task may depend on the specific choice of control electrodes. We hypothesize that output (i.e. BMI) electrodes can be decoupled if they record from separate cortical columns that are part of separable functional columnar networks, the existence of which has been postulated on computational grounds [17].

V. Conclusion

This work carries implications for the development of practical μECoG-based BMI, as it demonstrates the benefits of high-density electrode arrays and, at the same time, hints at a fundamental limit for the maximum useful spatial resolution (200 μm). The fact that sub-mm length scales can be decoupled through learning, could promote the development of clinically relevant, minimally invasive neural interfaces that do not break the blood-brain barrier and can be implanted through very small burr holes.

This study needs to be expanded to establish the significance of any trend in Fig. 5. Moreover, to test the hypothesis that columnar organization into micro-networks ultimately determines the minimum decoupleable length scale useful for μECoG-based BMI control, the correlation between target accuracy and cortical microanatomy below the control electrodes should be investigated.

Acknowledgment

P. L. thanks Nanoshift for assistance with cleanroom fabrication and Tim J. Blanche for providing the nanoZ.

References

[1] J. M. Carmena, M. A. Lebedev, R. E. Crist, J. E. O'Doherty, D. M. Santucci, D. F. Dimitrov, P. G. Patil, C. S. Henriquez, and M. A. L. Nicolelis, "Learning to control a brain-machine interface for reaching and grasping by primates.," *PLoS biology*, vol. 1, no. 2, p. E42, Nov. 2003.

[2] M. Mahmud, D. Hawellek, and A. Bertoldo, "EEG based brain-machine interface for navigation of robotic device," in *2010 3rd IEEE RAS & EMBS International Conference on Biomedical Robotics and Biomechatronics*, 2010, pp. 168–172.

[3] G. S. Brindley and M. D. Craggs, "The electrical activity in the motor cortex that accompanies voluntary movement.," *The Journal of physiology*, vol. 223, no. 1, p. 28P–29P, May 1972.

[4] W. J. Freeman, L. J. Rogers, M. D. Holmes, and D. L. Silbergeld, "Spatial spectral analysis of human electrocorticograms including the alpha and gamma bands," *Journal of Neuroscience Methods*, vol. 95, no. 2, pp. 111–121, Feb. 2000.

[5] M. W. Slutzky, L. R. Jordan, T. Krieg, M. Chen, D. J. Mogul, and L. E. Miller, "Optimal spacing of surface electrode arrays for brain-machine interface applications.," *Journal of neural engineering*, vol. 7, no. 2, p. 26004, Apr. 2010.

[6] J. Viventi, D.-H. Kim, L. Vigeland, E. S. Frechette, J. A. Blanco, Y.-S. Kim, A. E. Avrin, V. R. Tiruvadi, S.-W. Hwang, A. C. Vanleer, D. F. Wulsin, K. Davis, C. E. Gelber, L. Palmer, J. Van der Spiegel, J. Wu, J. Xiao, Y. Huang, D. Contreras, J. A. Rogers, and B. Litt, "Flexible, foldable, actively multiplexed, high-density electrode array for mapping brain activity in vivo.," *Nature neuroscience*, vol. 14, no. 12, pp. 1599–605, Dec. 2011.

[7] D. Khodagholy, T. Doublet, M. Gurfinkel, P. Quilichini, E. Ismailova, P. Leleux, T. Herve, S. Sanaur, C. Bernard, and G. G. Malliaras, "Highly conformable conducting polymer electrodes for in vivo recordings.," *Advanced materials (Deerfield Beach, Fla.)*, vol. 23, no. 36, pp. H268–72, Sep. 2011.

[8] A. G. Rouse, J. J. Williams, J. J. Wheeler, and D. W. Moran, "Cortical adaptation to a chronic micro-electrocorticographic brain computer interface.," *The Journal of neuroscience : the official journal of the Society for Neuroscience*, vol. 33, no. 4, pp. 1326–30, Jan. 2013.

[9] T. Blakely, K. J. Miller, S. P. Zanos, R. P. N. Rao, and J. G. Ojemann, "Robust, long-term control of an electrocorticographic brain-computer interface with fixed parameters.," *Neurosurgical focus*, vol. 27, no. 1, p. E13, Jul. 2009.

[10] A. C. Koralek, X. Jin, J. D. Long, R. M. Costa, and J. M. Carmena, "Corticostriatal plasticity is necessary for learning intentional neuroprosthetic skills.," *Nature*, vol. 483, no. 7389, pp. 331–5, Mar. 2012.

[11] P. Ledochowitsch, R. J. Felus, R. R. Gibboni, A. Miyakawa, S. Bao, and M. M. Maharbiz, "Fabrication and testing of a large area, high density, parylene MEMS," in *2011 IEEE 24th International Conference on Micro Electro Mechanical Systems*, 2011, pp. 1031–1034.

[12] J. Johnson, "Thermal Agitation of Electricity in Conductors," *Physical Review*, vol. 32, no. 1, pp. 97–109, Jul. 1928.

[13] H. Nyquist, "Thermal Agitation of Electric Charge in Conductors," *Physical Review*, vol. 32, no. 1, pp. 110–113, Jul. 1928.

[14] S. F. Lempka, M. D. Johnson, M. A. Moffitt, K. J. Otto, D. R. Kipke, and C. C. McIntyre, "Theoretical analysis of intracortical microelectrode recordings.," *Journal of neural engineering*, vol. 8, no. 4, p. 045006, Aug. 2011.

[15] C. RAO and D. TRIVEDI, "Chemical and electrochemical depositions of platinum group metals and their applications," *Coordination Chemistry Reviews*, vol. 249, no. 5–6, pp. 613–631, Mar. 2005.

[16] V. B. Mountcastle, "The columnar organization of the neocortex.," *Brain : a journal of neurology*, vol. 120 (Pt 4, pp. 701–22, Apr. 1997.

[17] P. Simen, T. Polk, R. Lewis, and E. Freedman, "Universal computation by networks of model cortical columns," in *Proceedings of the International Joint Conference on Neural Networks, 2003.*, vol. 1, pp. 230–235.